Shinsuke Oh-hara, et. al. International Journal of Engineering Research and Applications
www.ijera.com
ISSN: 2248-9622, Vol. 11, Issue 7, (Series-III) July 2021, pp. 29-36

RESEARCH ARTICLE OPEN ACCESS

Formation Control of Multiple Mobile Robots by Fisheye Camera

Shinsuke Oh-hara*, Seiya Matsushita, Atsushi Fujimori*
**(Department of Mechanical Engineering, University of Yamanashi, Japan*

ABSTRACT
In this paper, we consider a formation control of multiple mobile robots by fisheye cameras. By recognizing the surrounding mobile robot from the image information of cameras, formation control becomes feasible even if there is no information exchange by communication between robots. A fisheye camera has a wide viewing angle, enabling a wide range of object recognition, and is highly useful. However, the resulting image is distorted, in order to perform the position and posture estimation based on the marker recognition, it is necessary to consider the distortion of this image. On the other hand, it is easier to design the control system based on the physical quantity of position and speed than using the feature quantity of the image, when the formation control of multiple mobile robots is considered. In this paper, a fisheye camera is modeled based on spherical coordinates, and a position estimation method by marker recognition is proposed. Next, we propose a velocity estimation method for a leader robot based on a disturbance observer by using the obtained position information. In addition, we introduce a formation control method based on the virtual structure of mobile robots. The effectiveness of the proposed method is verified through experiments.

***Keywords*-**Formation control, Fisheye camera, Position and velocity estimation, Maker recognition, Disturbance observer.

Date of Submission: 05-07-2021 Date of Acceptance: 18-07-2021

I. INTRODUCTION

Recently, research on formation control of mobile robots has been actively performed. The purpose of formation control is to control multiple mobile robots so as to form a specific formation and perform autonomous driving while maintaining the formation. For example, it is applied to automatic platoon transportation such as multiple trucks, and can be expected to reduce transportation costs [1]. Various applications such as formation flight of an artificial satellite are considered.

In order to realize formation control of mobile robots, it is necessary to measure relative distance, velocity and attitude angle between robots, and to acquire their information of surrounding robots. There is a research that considers multiple mobile robots as multi-agents, and realize a specific team by exchanging information of each agent through a network constructed between multi-agents, considering a specific formation as a consensus problem between agents [2]. This study requires mutual communication between robots. On the other hand, Fujimori et al. [3] estimates the position of a leader robot based on distance information obtained from multiple sonars mounted on the mobile robot, and realizes the formation control considering obstacle avoidance, which does not require mutual communication between robots. Due to recent improvements in image processing technology, the formation control using cameras instead of distance sensors such as laser range finders and sonar sensors has been considered in [4], [5].

Many commonly available cameras use standard lenses. Though the camera equipped with the standard lens is close to the human visual field, in many cases, the visual field is narrow in order to apply it to the control of the mobile robot. A narrow field of view of the camera may result in losing sight of the object to be tracked. Furthermore, the object in the blind spot of the camera may not be recognized and collided with robots. For such problems, the introduction of omni-directional cameras has been considered, but the lenses have larger and more complex structures compared with commercially available webcams. That is, the omni-directional cameras are difficult to handle. There is also a problem that reliable omnidirectional cameras are expensive. On the other hand, in recent years, with the popularization of smartphones, fisheye lenses that can be attached to small cameras of smartphones and are inexpensive have become commercially available. This paper considers that the visual field of the camera is enlarged by attaching the fisheye lens to the camera, and the formation control based on the image information. However, since the image information obtained by the fisheye camera is distorted, it becomes difficult

to introduce the conventional image processing. The authors realize a visual feedback control law for a fisheye camera model and applies it to position control of a mobile robot [6].This method does not require physical information such as position, and it is a method to control a mobile robot only by the feature quantity of the image. On the other hand, when considering the formation control of multiple mobile robots, it is easier to construct the control system by utilizing physical information such as relative position and velocity.

This paper discusses a method for estimating the relative position and velocity of a robot tracking from image information obtained from a fisheye camera. In this paper, we propose a formation control method for mobile robots by fisheye cameras and verify it by experiments using two mobile robots. At first, we propose an estimation method of relative positions between robots from marker information by performing marker recognition with a fisheye camera using AR markers. Then, we consider leader-follower type formation control and constructs formation control based on virtual structure. In order to realize a good formation control, it is necessary to measure the velocity of the tracked vehicle (the leader robot) and use it as a reference input. Here, the velocity of the leader is estimated based on a nonlinear disturbance observer. Next, we show the experimental results of velocity estimation by a disturbance observer and formation control of two robots in order to evaluate the effectiveness of the proposed method. Finally, we summarize this paper.

II. POSITION ESTIMATION BY MARKER RECOGNITION USING A FISHEYE CAMERA

2.1 Fisheye camera model

The projection model of the camera of the standard lens is modeled based on the principle of the pinhole camera. In this principle, geometrical properties such as similarity of shapes of objects projected on an image plane are invariant. On the other hand, the fisheye camera is enlarged in the field of view, but the shape of the object is projected with distortion. Therefore, the geometrical properties of the shape of the object projected on the image plane are not kept in the fisheye camera model. To cope with the distortion of this image, a camera model utilizing spherical coordinates has been studied [7], [8], [9], [10], and the marker position estimation by spherical model is also considered in this paper.

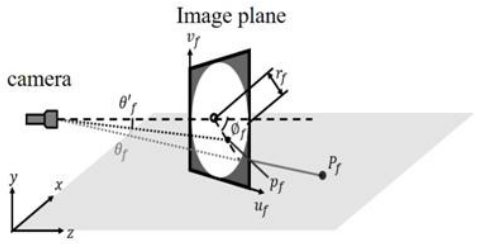

Figure 1. Fisheye camera model

Fig. 1 shows the projection model of the fisheye camera. Consider the case where the vector P_f from the camera coordinate systemis projected to the image vector p_f in the image plane of the fisheye camera. The perspective projection of the fisheye camera can be described by the angle θ_f between the optical axis and the projection line from the image point to the image plane, and the image height r_f on the plane. In this paper, the projection scheme of the fisheye camera is assumed to be described by the following approximation equation

$$r_f \approx f\left(\theta_f + k_1\theta_f^3 + k_2\theta_f^5 + k_3\theta_f^7 + k_4\theta_f^9\right) \quad (1)$$

where f is the focal length of the camera. Each coefficient k_1, k_2, k_3, k_4 in the equation (1) is a value derived by calibration and model radial aberrations.

Let $p_f = [u_f \quad v_f]^T$ be the coordinate position on the image plane of the fisheye camera, and $c = [c_u \quad c_v]^T$ be the optical axis point of the image plane. The image height r_f and the angle ϕ_f with u axis can be calculated by the following equation

$$r_f = \sqrt{\left(u_f - c_u\right)^2 + \left(v_f - c_v\right)^2} \quad (2)$$

$$\phi_f = \tan^{-1}\left(\frac{v_f - c_v}{u_f - c_u}\right) \quad (3)$$

In this paper, we consider to project an image obtained by the fisheye camera onto a spherical model with a radius of 1. Based on the image pointp_f, we can calculate the image height r_f and ϕ_f from the equations (2) and (3), substitute them into the equation (1) and solve the polynomial to obtain θ_f.

2.2 Position estimation using AR markers

We describe the position and posture estimation from the marker information recognized by the image processing. We assume that the marker is a square and the length of one side is known. Consider first that the feature quantity of the four corners of the first recognized marker is projected to a point on a spherical model of radius 1 as shown in Fig. 2.

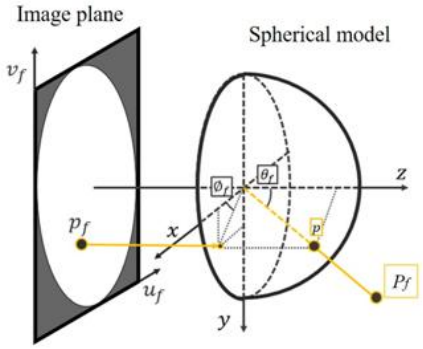

Figure 2. Spherical model

It is known that the following properties of figures projected on a spherical model are conserved from the literature[9].

(i) Linearity: A straight line in space becomes part of a great circle.

(ii) Parallelism: Multiple great circle groups made by parallel straight lines in space pass through one axis (parallel line projection axis) through the origin.

(iii) Orthogonality: The projection axes of two sets of orthogonal lines in space are orthogonal.

In this paper, the position estimation is performed from the marker recognition by utilizing these properties.

From ϕ_f and θ_f calculated form the equations (1) to (3), the image point p_f is projected to a point p on a spherical model of radius 1(see Figure 2). It can be expressed by the following equation

$$p = \left[\sin\theta_f \cos\phi_f \sin\theta_f \sin\phi_f \cos\theta_f\right]^T \quad (4)$$

Next, consider a plane containing the origin, p_i and p_{i+1}. The unit normal vector n_i of this plane can be expressed by the following equation

$$n_i = \frac{p_i \times p_{i+1}}{\|p_i \times p_{i+1}\|} \ (i = 1, \cdots 4) \quad (5)$$

where $\times$ is the cross product and $p_5 = p_1$. The multiple parallel lines projected on a spherical model pass through one axis (parallel projection axis) passing through the viewpoint [9]. The normal vector of the axis of parallel projection for the opposite sides of the square marker recognized from this property is obtained by the following calculation

$$\begin{cases} n_{r1} = \frac{n_1 \times n_3}{\|n_1 \times n_3\|} \\ n_{r2} = \frac{n_2 \times n_4}{\|n_2 \times n_3\|} \end{cases} \quad (6)$$

The projected lines of the two orthogonal lines also from orthogonality, so that the two normal vectors are also orthogonal. Since these two normal vectors are normal to the parallel projection axis, they can be regarded as representing the orientation of the marker. Therefore, the rotation matrix of the marker coordinate system viewed from the spherical model coordinate system is set as follows

$$R = [n_{r2} \quad n_{r1} \quad n_{r2} \times n_{r1}] \quad (7)$$

Next, we derive the translational vectors between the spherical model coordinate system and the marker coordinate system. The marker is square and its center of gravity is the origin of the marker coordinate system. Hence, the coordinate position of each vertex is expressed as shown in the equation (8)

$$\begin{cases} P_1 = [-\frac{l}{2} \ \ \frac{l}{2} \ \ 0\ ]^T \\ P_2 = [-\frac{l}{2} \ \ -\frac{l}{2} \ \ 0\ ]^T \\ P_3 = [\ \frac{l}{2} \ \ -\frac{l}{2} \ \ 0\ ]^T \\ P_4 = [\ \frac{l}{2} \ \ -\frac{l}{2} \ \ 0\ ]^T \end{cases} \quad (8)$$

The relationship between the maker point P_i and the corresponding point p_i in the spherical model can be expressed by the rotation matrix R and the translation vector T as follows

$$\zeta_i \begin{bmatrix} p_i \\ 1 \end{bmatrix} = RP_i + T \ (i = 1, \cdots 4) \quad (9)$$

where ζ_i is a variable parameter that represents the scaling. Similar equations can be derived for the four points, and these can be solved as the following simultaneous equations for the translation vector T

$$\begin{bmatrix} -I_3 & p_1 & p_2 & p_3 & p_4 \end{bmatrix} \begin{bmatrix} T \\ \zeta_1 \\ \zeta_2 \\ \zeta_3 \\ \zeta_4 \end{bmatrix} = \begin{bmatrix} l(-n_{r1} + n_{r2})/2 \\ l(-n_{r1} - n_{r2})/2 \\ l(n_{r1} - n_{r2})/2 \\ l(n_{r1} + n_{r2})/2 \end{bmatrix} \quad (10)$$

In this paper, the robot is equipped with a USB camera, and a fisheye lens is attached to the camera. Calibration is performed using a camera calibration for a fisheye lens on OpenCV, and the focal length f, k_1, k_2, $k_3$and k_4 in the equation (1) are obtained. A marker is attached to the back of the leader robot, and the relative position between the robots are estimated by marker recognition. ArUco [11] is utilized for marker recognition. Fig. 3 shows a case in which an AR marker is mounted on the leader robot and the marker is recognized by the fisheye camera. We confirm that the position estimation between the marker and the camera is possible by the proposed method. It has also been experimentally found that a marker can be recognized if it is within the viewing angle of 80[deg] of the camera.

(a) The mobile robot and AR marker

(b) The fisheye camera image

Figure 3. Marker recognition with a fisheye camera

III. VELOCITY ESTIMATION AND FORMATION CONTROL WITH NONLINEAR DISTURBANCE OBSERBER

3.1 Velocity Estimation with Nonlinear Disturbance Observer

In order to realize a formation control in which multiple robots are driving while maintaining a specific shape, it is necessary to control not only the relative position between robots but also the same speed as the leader robot. In this paper, we consider a method for estimating the velocity of other mobile robots based on the relative position information of the robot itself, rather than the mutual information exchange between the robots.

The mobile robot used in this paper is a two-wheeled vehicle type and has non-holonomic constraints. Therefore, the relative motion of the two robots is a nonlinear system. We use a nonlinear system disturbance observer[12]in order to estimate the velocity of the leader robot.

Consider the following nonlinear affine system

$$\begin{cases} \dot{x} = f(x) + g_1(x)u + g_2(x)d \\ y = h(x) \end{cases} \quad (11)$$

where x, u, d and y are the state, input, disturbance and output of the system, respectively. We assume that $\dot{d} = 0$, the functions f , g_1 and g_2 are sufficiently smooth. Under these assumptions, the disturbance vector is estimated by the following equations

$$\begin{cases} \dot{z} = -L_d(x)g_2(x)z - L_d(x)(f(x) + g_1(x)u \\ \qquad +g_2(x)p(x)) \\ \hat{d} = z + p(x) \end{cases} \quad (12)$$

where z, $\hat{d}$ and $p(x)$ are the state vetor, estimated disturbace and auxiliary vector of the observer, respectively. $L_d(x)$ denotes the observer gain.

Based on the disturbance observer for the above nonlinear system, we consider the relative motion of a mobile robot (leader robot) to be tracked and a tracking mobile robot (follower robot). The relative motion of two mobile robots can be expressed as follows

$$\begin{bmatrix} \dot{e}_x \\ \dot{e}_z \end{bmatrix} = \begin{bmatrix} 0 & -e_z \\ -1 & e_x \end{bmatrix} \begin{bmatrix} V \\ \omega \end{bmatrix} + \begin{bmatrix} V_{rx} \\ V_{rz} \end{bmatrix} = g_1(e)u + V_r \quad (13)$$

where V and ω are the translational velocity and angular velocity of the follower robot, respectively. V_{rx} and V_{rz} are the velocities of the leader on the marker in the X and Z directions, respectively, we consider these as a disturbance vector. $e = exezT$ is the relative position vector in the obtained fromthe position estimation by the fisheye camera in the previous section. Assuming that the velocity of the leader changes in steps, the velocity is estimated by the disturbance observer in equation (14) below

$$\begin{cases} \dot{z} = -L_d z - L_d(g_1(e)u + p(e)) \\ p(e) = L_d e \\ \hat{V} = z + p(e) \end{cases} \quad (14)$$

3. 2 Formation Control Based on Virtual Structure

In this paper, we realize a formation control by using virtual structure [13]. We consider a marker is mounted on the leader robot, and a mobile robot is set virtually at a fixed distance from the follower robot as shown in Fig. 4. The desired formation can be formed by controlling the center of gravity of this virtual robot to match the position and velocity of the marker.Let $l = [l_x \quad l_z]^T$ be the designated formation positions of the follower robot. The relative error between the marker point of the leader and the center of gravity of the virtual robot is $\tilde{e} = [\tilde{e}_x \quad \tilde{e}_z]^T$, and the velocity of the marker point is $V_r = [V_{r_x} \quad V_{r_z}]^T$.

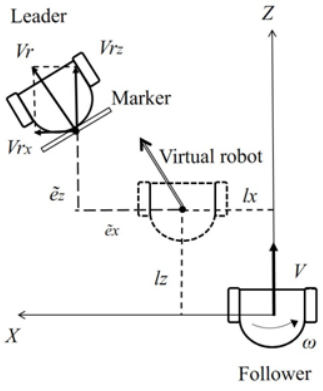

Figure 4. Virtual structure of mobile robot

We calculate the velocity V and angular velocity ω, which are the control inputs for the follower to make the center of gravity of the virtual robot coincide with the marker point based on the following equations

$$\begin{cases} \omega = \frac{V_{r_x} - k_x \tilde{e}_x}{l_z} \\ V = V_{r_z} - k_z \tilde{e}_z + \frac{V_{r_x} - k_x \tilde{e}_x}{l_z} l_x \end{cases} \quad (15)$$

The parameters k_x and k_z are the control gain. Equation (15) requires the velocity of the leader but here we use the velocity of the leader estimated by the disturbance observer. Thus, the desired formation is realized, and good tracking performance can be expected by utilizing the estimated speed. A block diagram of the control system of the proposed method is shown in Fig. 5.

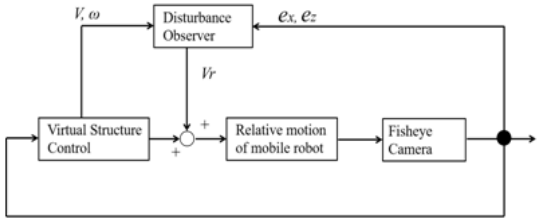

Figure 5. Block diagram of formation control System

IV. EXPERIMENTAL VERIFICATION

This paper evaluates the effectiveness of the proposed method using two mobile robotic Pioneer3DX platform. In the experiment, the two robots were arranged as shown in Fig. 6. First, this paper verifies velocity estimation of linear motion by the disturbance observer, and then conducts a formation control experiment when the leader robot makes linear motion and curved motion.

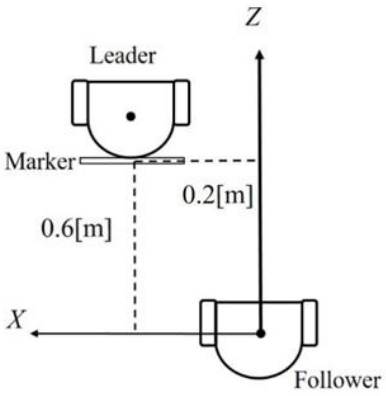

Figure 6. Initial placement of the robots

4.1 Velocity Estimation by Disturbance Observer

In the experiment of velocity estimation, the estimation accuracy of the disturbance observer is verified by moving the mobile robot straight ahead. In this paper, we give a speed command to each robot and move it without formation control to the mobile robot. The disturbance observer gain L_d in Equation (14) is set to 0.4. Then, the same translational velocity command $V_l = V_f = 0.100$[m/s] is given to each robot so that the two robot are moved straight. V_l and V_f are the translational velocity of the leader and follower, respectively. Fig.7 shows the velocity estimation results and the relative position between the robots. In this velocity estimation experiment, the estimated vector of the disturbance observer converges to$\hat{V} = [0 \quad 0.105]^T$. The relative distance between the robots is increased with respect to the Z direction. Calculating the speed of each mobile robot from the distance and time traveled, the leader is traveling at the speed of 0.105 [m/s] and the follower is traveling at 0.103 [m/s]. This experiment shows that the velocity estimation based on the disturbance observer has good accuracy, and it is possible to estimate the relative position during motion.

4.2 Case of linear motion

Next, in order to verify the effectiveness of the proposed method, we conducted an experiment of formation control when the leader moved straight. The gain of the control law in Equation (15) is set to $k_x = 2.0$ and $k_z = 0.35$, respectively. In the experiments, the robots are placed at the initial position shown in Fig.6 and then only the follower is moved to the target formation shape $l = [l_x \quad l_z]^T = [0.2 \quad 0.5]^T$ by using the formation control. After that, the leader is moved to in linear motion with $V_l = 0.100$ [m/s]. Experimental results of linear motion are shown in Fig. 8 and 9.

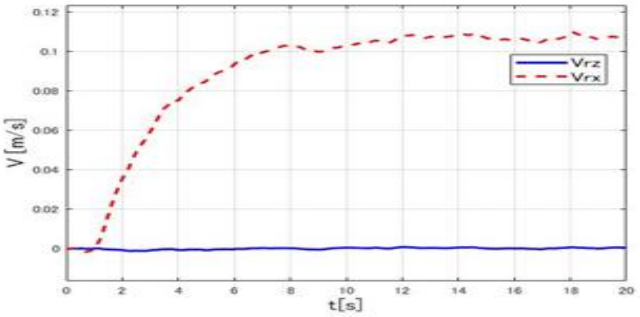

(a) Estimated velocities

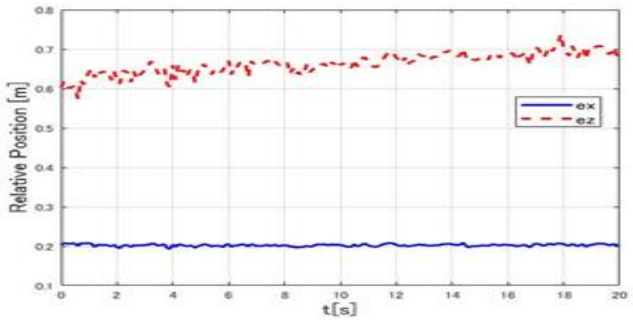

(b) Relative positions

Figure 7. Experimental results of the velocity estimations

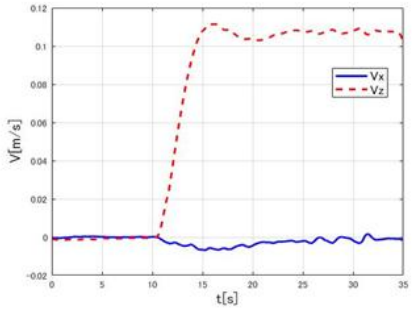

(a) Estimated velocities

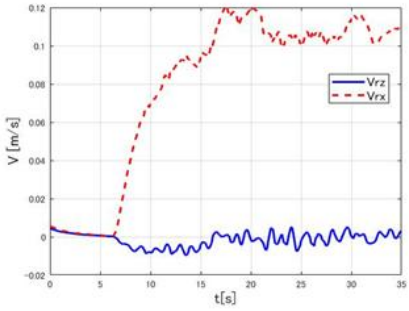

(a) Estimated velocities

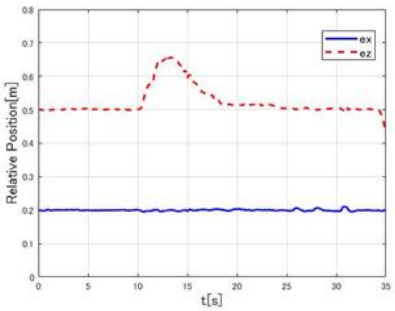

(b) Relativepositions

Figure 8. Experimental results of the formation control with disturbance observer

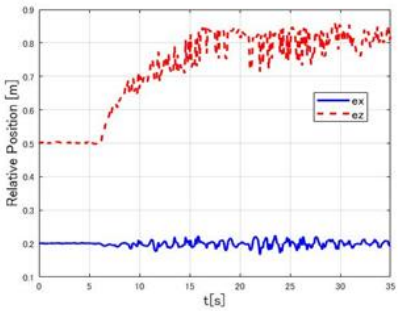

(b) Relativepositions

Figure 9. Experimental results of the formation control without disturbance observer

From Fig.8 (a), the estimated velocity V_z can be seen that it converges to 0.10 [m/s]. The relative positions in the X and Z directions converge to 0.2m and 0.5m, respectively, and the desired formation is formed, indicating that it can follow the leader. For comparison, the experimental results when only virtual structure formation control is used are shown in Fig. 9. Note that a disturbance observer estimated the speed, but the estimated value was not used for formation control. In the experiment, the relative position in the Z direction has a value of 0.8[m]. This indicates that the virtual structure formation control is a proportional control, and thus requires an error with the formation shape to run in formation.On the other hand, in the proposed method, an error occurs in the formation shape when the leader starts to move, but the target formation shape is realized by adding the speed estimated by the disturbance observer and the virtual structure formation control law. The experimental results show the effectiveness of the proposed method.

4.3 Case of curvilinear motion

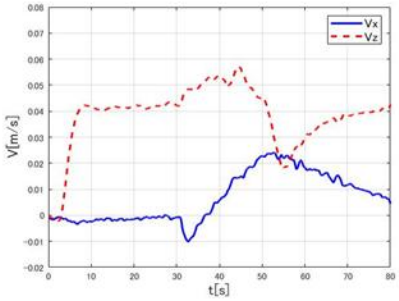

(a) Estimated velocities

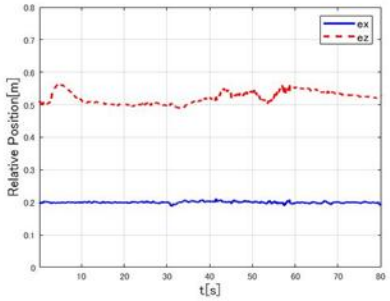

(b) Relativepositions

Figure 10. Experimental results of the formation control in curvilinear motion

Next, the experimental result of the curved motion of the leader is shown. Here, the translational velocity and turn angular velocity of the leader are $V_l = 0.05$ [m/s] and $\omega_l = 4$ [deg/s], respectively. Initially, the robot is moved in a straight line motion, then the robot is rotated about 90[deg], and then it is moved in a straight line motion again. The results of velocity and relative position estimation during curvilinear motion are shown in Fig. 10 and 11. Fig. 11 shows the trajectories of the leader and follower robot obtained by the odometry of Pioneer3DX. The dash line is the trajectory of the marker with the relative positions shown in Fig. 10(b) added to the trajectory of the follower. Fig. 12 shows how the marker was recognized by the fisheye camera. The follower tracks the leader while maintaining the target shape, but there is an error in the formation with respect to the Z direction during the curvilinear motion.

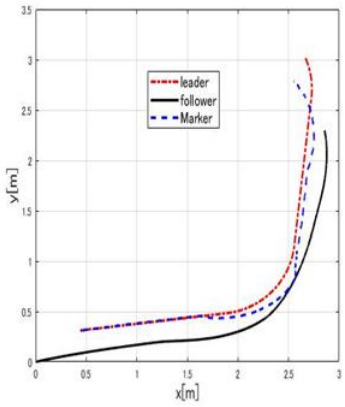

Figure 11. The trajectories of the leader and follower robot

Figure 12. The snapshots of marker recognition by fisheye camera.

This is probably because the velocity of the leader fluctuated during the motion and it took time for the velocity estimate by the disturbance observer to converge. It can be seen from the above that in the curvilinear motion, the error of the formation shape occurs a little, but it shows the good tracking performance.

V. CONCLUSIONS

In this paper, a formation control of multiple mobile robots using a fisheye camera is realized. First, a fisheye camera is regarded as a spherical model, and a position estimation method based on the model is realized. Next, we construct the formation control system which combines velocity estimation of a mobile robot with a nonlinear disturbance observer and tracking control based on a virtual structure. The effectiveness of the proposed method is shown by experiments of formation control using two mobile robots. Good formation control is realized by the proposed method.

As future problems, it is to develop a formation control method which does not require position estimation of markers and marker recognition suitable for fisheye cameras, and to enable recognition of robots in a wider range.

ACKNOWLEDGEMENTS

This work was supported by JSPS KAKENHI Grant-in-Aid for Scientific Research(C) 18K04046.

REFERENCES

[1]. New Energy and Industrial Technology Development Organization (NEDO), NEDO's Research and Development Achievements on ITS, http://www.nedo.go.jp/content/100552007.pdf 2013.

[2]. A. Yoshioka and T. Namerikawa, Consensus Problem for Multi-agent System and Its Application to Formation Control. *Transactions of the Society of Instrument and Control Engineers*, 44(8), 2008, 663-669.

[3]. A. Fujimori, A. Hosono, K. Takahashi and S. Oh-hara, A Modified Navigation Technique for Formation Control of Sonar-Equipped Mobile Robots with Large Obstacle Avoidance, *International Journal of Modern Engineering Research*, 8(9), 2019, 44-52.

[4]. S. Oh-hara, M Ohmura, K. Saito and A. Fujimori, Formation Control for Multiple Mobile Robots Using Visual Information. *The Proceedings of the Conference on Information, Intelligence and Precision Equipment: IIP*, Tokyo, Japan, 2017, G-04.

[5]. X. Liang, H. Wang, YH. Liu and W. Chen, Formation Control of Nonholonomic Mobile RobotsWithout Position and Velocity Measurements. *IEEE Transactions on Robotics*, 34(2), 2018, 434-446.

[6]. S. Oh-hara, T. Isogai T and A. Fujimori, Visual Feedback Control for a Mobile Robot with a Fish-Eye Camera. *The 62nd Annual Conference of the Institute of Systems, Control and Information Engineers*, Kyoto, Japan, 2018, 213-2.

[7]. Kannala J and Brandt SS. A Generic Model and Calibration Method for Conventional. Wide-Angle, and Fish-eye Lenses. *IEEE Transactions on Pattern Analysis and Machine Intelligence,* 28(8), 2006, 1335-1340.

[8]. S. Kase, R. Okutsu, H. Mitsumoto, Y. Aragaki, N. Shimomura, K. Terabayashi and K. Umeda, A method to Construct Overhead View Images Using Multiple Fish-Eye Cameras. *Journal of the Japan Society of Precision Engineering*, 75(2), 2009, 251-255.

[9]. H. Komagata, I. Ishii, A. Takahashi, D. Wakatsuki and H. Imai, A Geometric Calibration Method of Internal Camera Parameter for Fish-Eye Lenses, *The IEICE transactions on information and systems (Japanese edition)*, J89-D(1), 2006, 64-73.

[10]. M. Nakano, S. Li and N. Chiba, Calibrating Fisheye Camera by Stripe Pattern Based upon Spherical Model, *The IEICE transactions on information and systems (Japanese edition)*, J90-D(1), 2007, 73-82.

[11]. S. Garrido-Jurado, R. Munoz-Salinas, F.J. Madrid-Cuevas and M. J. Marin-Jimenez, Automatic Generation and Detection of Highly Reliable Fiducial Markers under Occlusion. *Pattern Recognition*, 47(6), 2014, 2280-2291.

[12]. A. Mohammadi, HJ. Marquez and M. Tavakoli, Non-linear Disturbance Observers: Design and Applications to Euler-Lagrange Systems, *IEEE Control Systems Magazine*, 37(4), 2017, 50-72.

[13]. I. Ikeda, J. Jongusuk, T. Ikeda and T. Mita, Formation Control of Multiple Nonholonomic Mobile Robots, *IEEJ Transactions on Industry Applications*, 124(8), 2004, 814-819.